Decohesion with Gap Closure and Refreezing

Kara Peterson[a,1], Howard Schreyer[b], Deborah Sulsky[c,*]

[a] *Sandia National Laboratories, Albuquerque, NM*
[b] *Department of Mechanical Engineering, MSC01 1150, 1 University of New Mexico, Albuquerque, NM 87131*
[c] *Department of Mathematics and Statistics, MSC01 1115, 1 University of New Mexico, Albuquerque, NM 87131*

Abstract

In previous work, an elastic-decohesive constitutive model was developed for sea ice. The model predicts the initiation of leads and provides their orientation. Moreover, the model indicates how a lead will open and close depending on the environment in which it is forced. However, once a lead is formed, it persists indefinitely and can open and close without resistance. This paper builds on that previous work and suggests enhancements to the model to include two new features. First, if ice freezes within a lead, we add resistance to closing the gap. Second, if the lead closes and is stationary, we add the possibility that the lead will refreeze and resist further opening. These features are included in a sample numeric calculation to demonstrate their effect.

Keywords: decohesive constitutive model, sea ice, fracture, refreezing, gap closure

1. Introduction

Sea ice mediates the heat transfer between the ocean and atmosphere. In the winter, sea ice acts to insulate the warmer ocean water from the colder atmosphere. Ice motion is driven by oceanic currents and atmospheric winds. In order to move, the ice cover continuously breaks up and refreezes. The leads, or cracks in the ice, can be kilometers wide and up to hundreds of kilometers long. The importance of leads in modeling sea ice is well known. New ice is formed primarily in leads where open water, exposed to the cold atmosphere, freezes quickly. As leads close, ice piles up into pressure ridges, or is forced down into keels, creating thicker ice. In addition, the greater albedo of the ice compared to the water results in more reflected solar radiation and cooler ice, sea, and air surface temperature. The process of freezing sea water to form ice, also results in brine ejection. Thus, leads additionally dominate the brine flux into the ocean mixed layer, which alters ocean circulation. Climate simulations strive to capture these important effects of leads.

Current sea-ice models have three major components. The first component models the ice dynamics, that is, its motion. Ice dynamics is governed by the momentum equation which expresses the physical principle

*Corresponding Author

[1] Sandia National Laboratories is a multi-program laboratory managed and operated by Sandia Corporation, a wholly owned subsidiary of Lockheed Martin Corporation, for the U. S. Department of Energy's National Nuclear Security Administration under Contract DE-AC04-94AL85000.

(Newton's 2nd law) that changes in momentum of an object occur due to forces acting on the object. The forces acting on the ice are drag from the wind and ocean, Coriolis forces, gravitational effects from the sea surface tilt, and internal ice forces that follow a constitutive model. The second component models ice thermodynamics, and is governed by a heat equation describing the temperature of the ice and snow through the thickness. The third component is an ice thickness distribution. The ice thickness distribution is a subgrid parameterization of the spatial heterogeneity of the ice thickness and accounts for redistribution of ice due to lead opening and closing. Thus, the constitutive model is one piece of a comprehensive ice model which accounts for the internal forces in the ice. These forces are responsible for the observed deviation in ice motion from free drift and, as noted, are especially important in the winter. The full set of equations is given in Appendix A.

To account for the presence of leads, a decohesive constitutive model was developed for predicting the initiation and opening of leads in the Arctic ice (Schreyer et al., 2006). Once the existence of leads is taken into account, the remaining motion of the ice has small deformations and is appropriately described as elastic. The phrase elastic-decohesive is used to describe this model of the dual continuum-discontinuum aspects of the behavior of Arctic ice. Several features were designed into the model. First, the model was constructed to predict the observed features of transition from brittle failure under tensile to moderate values of compression, to mixed modes of failure under larger compression, and to a plastic-like faulting under large confinement (Schulson, 2004). The various modes of failure occur in the model, depending on the stress state in the material. In other words, the predicted mode of failure depends on the state of stress, a feature not contained in most other models. Where the transitions occur in stress space depends on the material parameters and can be adjusted based on empirical data. Second, the model can handle multiple cracks at a point, and therefore can predict crack branching. Third, the numerical implementation of the model is accomplished similarly to standard plasticity models. Thus, in principle, modular codes that call a subroutine to implement the constitutive model can substitute the elastic-decohesion model if it proves worthwhile. A final aspect of the model is the ability to build in initial planes of weakness that may be due to pre-existing, partially frozen leads, for example. Initial tests of the model on a regional simulation of the Beaufort Sea show that the model is able to capture the qualitative and statistical behavior of localized deformation seen in satellite observations (Sulsky and Peterson, 2011). This constitutive model is described in detail in Section 2.

Preliminary tests on basin-scale simulations of the Arctic, over a season or more, indicate that more opening and fracture of the ice is predicted than what is calculated by processing satellite images. Sulsky and Peterson (2011) also note more fractures in their regional model. We postulate that a primary reason for these results is that in the current model, leads can close mechanically but their strength is not adjusted if they close and refreeze. Moreover, there is no resistance to closing or reopening once a lead has fully formed. Similarly, ice can grow in open leads due to thermodynamic processes, but the new ice does not as yet result in an adjustment to the ice strength. This paper introduces modifications to the elastic-decohesive model to

account for these aspects of ice behavior. In the next section of the paper, we review the elastic-decohesive model to date. In Section 3, we address the new model features and then in Section 4 we illustrate, in numeric examples, the implication of these features. Finally, in Section 5 we give concluding remarks.

2. The Elastic-Decohesive Model

The ice is modeled as elastic until a stress threshold is reached, in which case the ice can fail and form a lead. For the purposes of modeling sea ice, a two-dimensional, plane-stress description of failure has been formulated assuming cracks occur in the plane. The envelope of failure points in stress space is described by a failure function, $F_n(\boldsymbol{\sigma}, \mathbf{n})$ where $F_n < 0$ implies no failure, $F_n = 0$ implies evolving failure and $F_n > 0$ is not allowed. This function is analogous to a plastic yield function in plasticity theories. The subscript n on F_n indicates a separate failure function for each potential crack orientation, and F_n depends on the stress $\boldsymbol{\sigma}$, and the unit normal $\mathbf{n}$ to the crack surface. To consider all possible failure directions, a general failure function F is defined as $F = \max_n F_n$.

Many classical failure criteria, such as the Rankine, Tresca and Mohr-Coulomb criteria, are expressed in terms of the traction on the failure surface (i.e., crack surface). The elastic-decohesion model extends these classic criteria by adding two new features: (1) a modification of the Rankine criterion for brittle failure to allow for the possibility that a compressive stress component may lower the resistance of the material to brittle failure, and (2) a transition from brittle to ductile failure within one criterion. If a local basis consisting of $\mathbf{n}$, the unit normal to the crack, and $\mathbf{t}$, a unit vector tangent to the crack, is introduced, then the traction on the failure surface has normal component $\tau_n = \mathbf{n}\cdot\boldsymbol{\sigma}\cdot\mathbf{n}$ and tangential component $\tau_t = \mathbf{t}\cdot\boldsymbol{\sigma}\cdot\mathbf{n}$. The remaining component of stress in this basis (within the plane of the ice sheet) is the tangential stress, $\sigma_{tt} = \mathbf{t}\cdot\boldsymbol{\sigma}\cdot\mathbf{t}$. The brittle decohesion function is defined as follows

$$B_n = \frac{\tau_n}{\tau_{nf}} - f_n\left[\frac{\langle -\sigma_{tt}\rangle}{f_c'^2} + 1\right], \qquad \text{where } \langle x\rangle \equiv \begin{cases} x & x \geq 0 \\ 0 & x < 0 \end{cases}. \tag{1}$$

Material parameters are τ_{nf}, the tensile or normal failure stress and f_c' which denotes the failure stress in uniaxial compression. For the moment, take $f_n = 1$. The new criterion for brittle failure is $B_n = 0$. The McCauley bracket is used to activate the normal component of stress σ_{tt} only if it is negative. If the term involving σ_{tt} were absent then failure would occur when the normal traction on the surface reaches the threshold τ_{nf}, which is the Rankine criterion. With the σ_{tt} term, this criterion is analogous to the Rankine criterion in that failure occurs in the direction of maximum principal stress, but the critical value of the normal traction component is potentially reduced when σ_{tt} is compressive. The criterion allows for failure even if τ_n is negative, and it is this aspect of the model that allows compressive brittle failure.

Next, brittle and ductile aspects of failure are included by defining the failure function as

$$F = \max_n F_n \qquad F_n = \frac{\tau_t^2}{\tau_{sm}^2} + e^{\kappa B_n} - 1. \tag{2}$$

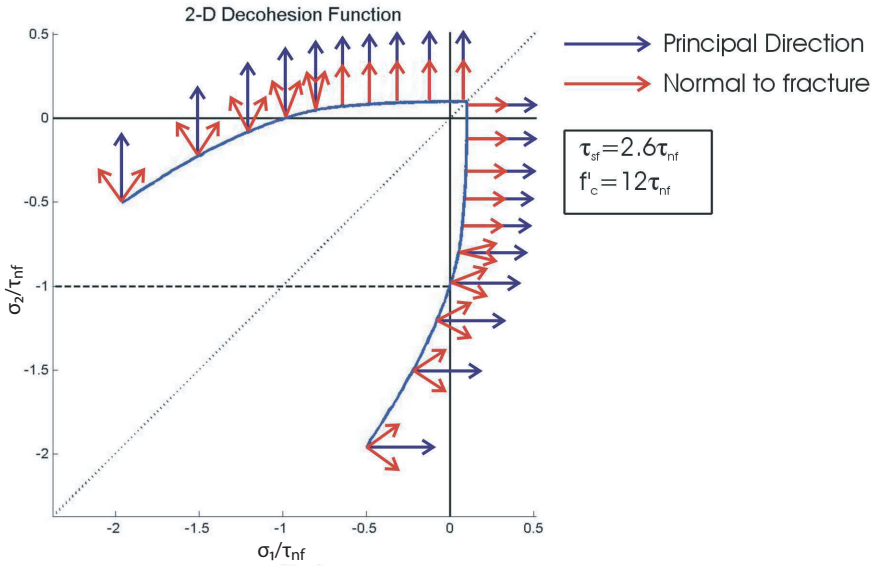

Figure 1: Failure envelope in principal stress space for the elastic-decohesive model.

The additional material parameter, τ_{sm}, is the failure stress in shear when the material is under large compression ($\tau_n \to -\infty$). The parameter, κ, is derived from the condition that under pure shear failure ($B_n = -1$), the failure stress is τ_{sf}, the failure stress under pure shear. If $\tau_{nf} \to \infty$ and $f'_c \to \infty$ then the criterion $F = 0$ reduces to the pure shear criterion of Tresca. Figure 1 shows a sketch of the decohesion failure envelope in stress space. This function is analogous to a yield function in plasticity theories. The solid line represents the failure envelope $F = 0$. Along this solid line, the blue arrows indicate the direction of maximum principal stress and the red arrows indicate the normal to the crack surface. Under brittle failure the normal to the crack is in the direction of maximum principal stress. Under ductile and mixed-mode failure the normal to the crack is at an angle to the direction of maximum principal stress, with two orientations of the crack possible. Of the two, the orientation that preserves the sense of local rotation is chosen. The transition from brittle to ductile failure occurs at a point along the failure envelope determined by the ratio of τ_{nf} to τ_{sf}, and thus is a material property.

This failure envelope describes the model for lead initiation in the ice. Once the beginning of a crack has been identified, the evolution of the lead is required. The term *decohesion* or *cohesive crack* model refers to the reduction of the traction on the crack as the crack opens. Decohesion is included in the model by introducing a softening parameter, analogous to equivalent plastic strain in plasticity models, that drives the traction to zero as a crack continues to open. A dimensionless parameter, f_n in Eq. 1, starts with a value unity for undamaged material and reduces to zero as u_n, the normal component of the jump in displacement, increases from zero. The crack is considered completely open when u_n reaches the material-dependent value u_0, at which point the traction on the crack surface has been reduced to zero and a free surface is thus formed. Accordingly, we set

$$f_n = \langle 1 - u_n/u_0 \rangle. \tag{3}$$

The displacement discontinuity evolves according to a normal flow rule

$$\dot{u}_n = \dot{\omega}\frac{\partial F}{\partial \tau_n} \qquad \dot{u}_t = \dot{\omega}\frac{\partial F}{\partial \tau_t}, \tag{4}$$

where a superposed dot indicates a time derivative. The displacement discontinuity is regularized into an effective decohesion strain, analogous to plastic strain,

$$\dot{e}^d_{nn} = \dot{u}_n/L \qquad \dot{e}^d_{nt} = \dot{u}_t/2L \qquad \dot{e}^d_{tt} = 0 \tag{5}$$

where L is a measure of the cell size in numerical simulations. (The value of L is chosen so that the physically correct energy is dissipated during fracture.) The stress is a function of the elastic strain $\mathbf{e} - \mathbf{e}^d$. Thus, as a specimen of ice is loaded, we typically begin with $F < 0$; the stress is inside the failure envelope. We assume each loading step is elastic, giving a trial stress state. If the trial stress is outside the failure envelope ($F > 0$) then a jump in displacement is introduced to bring F back to zero. This procedure is identical to standard solution procedures for plasticity. The result is that as a crack opens we predict the amount of both the normal and tangential opening. Once a free surface has formed, the jump in displacement can continue to grow if the crack surfaces continue to separate, and the traction on the surface remains zero.

At each loading step we find the critical direction $\mathbf{n}$ for which F is largest. As a crack with a particular orientation begins to open, the softening makes it likely that this orientation will remain the critical direction. However, it is possible that a changing stress state will make another direction critical, in which case a second crack can form intersecting the first. In this manner, the model accommodates multiple cracks at a point. If weak areas are known to exist in the ice, the softening parameter f_n can be initialized with a value less than one to account for this information.

3. Gap Closure and Refreezing

Our previous work, outlined in the last section, focuses on the prediction of lead formation. The model indicates the level of stress needed to form a lead. In addition, the model provides the orientation of the lead and tracks the amount of lead opening in terms of both the normal and tangential components of displacement associated with the displacement jump. The model above also allows for lead closure, but with no resistance to that closure. That is, once a lead is fully formed and the crack is defined by two free surfaces, those surfaces are free to move - either to open more or close, as conditions permit. However, as new ice is formed in an open lead, we expect the ice strength to begin to recover, and to resist further opening or closing of the lead. When the new ice is thin, the strength of the new ice is negligible in either tension or compression. With sufficient time and favorable thermodynamic conditions, a combination of freezing or crushing of ice in the lead builds up the thickness and the strength. This section of the paper focuses on the mechanical aspects of strength recovery due to refreezing and presents simple adjustments that extend the decohesive constitutive model to include physics of Arctic ice not present in the original model.

The thermodynamic model described in Appendix A tracks thickness changes in the ice due to freezing or melting. Moreover, the range of ice thickness within a computational cell that can be created by freezing

and ridging of ice is tracked by the ice thickness distribution model of Appendix A. When a lead is formed, open water is created and when a lead closes, ridging occurs and ice is redistributed from thinner to thicker ice in the thickness distribution. We assume that the thinnest ice in the ice thickness distribution occurs in a lead if one, or more, exists within a computational cell.

A simple approach to adding a gap closing force to the model would be to have the normal component of the resultant stress (force per unit length of the lead) be related to the normal component of the jump in displacement associated with the lead. For example, if g denotes the normal component of the resultant stress, then set

$$g = \sigma_g\big(1 - \frac{1}{\bar{u}^m}\big), \qquad \bar{u} = u_n/u_{\max}, \tag{6}$$

where $\sigma_g < 0$, a reference resultant compressive stress, and m, the exponent, are material constants. Recall that the normal component of the displacement jump is u_n. If a lead has opened to a distance $u_{\max}$, the current maximum opening of the lead producing new ice, then this value is used to non-dimensionalize the displacement jump.

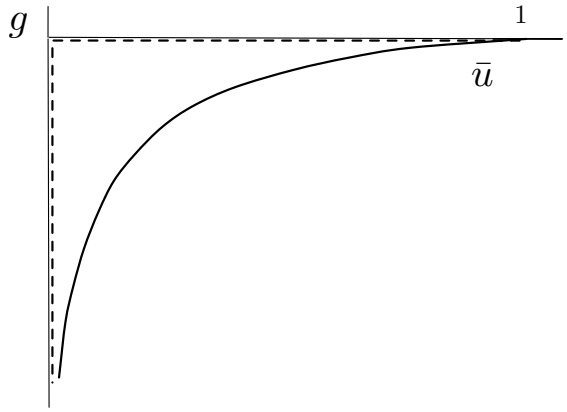

Figure 2: Possible forms for the gap closing force in terms of the normal component of the resultant stress, g, and the non-dimensional normal component of lead opening $\bar{u}$. The dashed line sketches the originally idealized model which offers no resistance to closing until the free surfaces forming the lead contact at zero width. The solid line sketches the smooth behavior represented by Equation 6.

Figure 2 contrasts the idealized approach used in the original model with the gap closing force given in Equation 6. The original model allows the gap to close from a scaled value of one down to zero without resistance. There is a normal component of resultant stress only when the two free surfaces making up the lead close sufficiently to come back into contact. The closing relation embodied in Equation 6 introduces a smooth closing force that is small when the lead is open and increases as the lead closes. Presumably, the lead would close under this relation until a ridge was completely formed by crushing any ice that existed in the lead. Because some ridged ice could remain in the lead, it would not be necessary for $\bar{u}$ to reach zero.

To further enhance the model, we consider that a lead can regain its strength if the lead closes and the free surfaces come together for a sufficient duration to refreeze. A change in strength in the ice model is

reflected by replacing the softening function f_n in Equation 3 with $\hat{f}_n$ where

$$\hat{f}_n = \begin{cases} \langle 1 - u_n/u_0 \rangle & \text{if the lead is opening or closing} \\ \hat{\tau}_{\mathrm{d}} & \text{if a lead has closed and } u_n \leq u_0 \end{cases}. \tag{7}$$

The new parameter, $\hat{\tau}_{\mathrm{d}}$, only becomes active once a lead has opened and closed. In intact ice, we start with no opening, $u_n = 0$, and $\hat{\tau}_{\mathrm{d}} = 0$. Thus, we have the original model where $\hat{f}_n = f_n = \langle 1 - u_n/u_0 \rangle$. A lead is formed when u_n reaches u_0 and the lead typically opens to a distance $u_n > u_0$. The original softening function, f_n, is zero once $u_n \geq u_0$. The value of $\hat{\tau}_{\mathrm{d}} = 0$ is unchanged until a ridge is formed. Suppose a lead opens to a width $u_n >> u_0$, ice now begins to form in the lead as water freezes. Further suppose conditions change so that the lead begins to close. If the lead closes completely, then u_n will return to a value equal to u_0. During this process, ridging takes place. Under stable conditions, the ridge will freeze and the ridged ice in the lead should regain strength. To accomplish this strengthening of the ice, an evolution equation for the growth of $\hat{\tau}_{\mathrm{d}}$ is proposed. Its value should start at zero and increase as freezing occurs. If $\hat{\tau}_{\mathrm{d}} < 1$, the inherent strength as given by $\hat{f}_n$ is less than the original material, but greater than the strength of the fully opened lead. Once $\hat{\tau}_{\mathrm{d}} = 1$, the lead has healed completely. The parameter $\hat{\tau}_{\mathrm{d}}$ does not increase beyond unity. At this point the lead is closed, u_n and $\hat{\tau}_{\mathrm{d}}$ are reset to zero, and the process can repeat.

Starting from the value zero, the rate of increase of strength, $\dot{\hat{\tau}}_{\mathrm{d}}$, is assumed to depend on the temperature difference between the air and the ocean. As the strength increases, it is possible that the rate decreases. Moreover, the strength should never exceed the original strength. Therefore, the following evolution equation is proposed

$$\dot{\hat{\tau}}_{\mathrm{d}} = \frac{A(T)}{(1 + \hat{\tau}_{\mathrm{d}})^m} \qquad \hat{\tau}_{\mathrm{d}}(0) = 0. \tag{8}$$

In this evolution equation, the parameter $A(T)$ is a ratio of the temperature difference between the ocean and air and a given reference temperature T_{ref} and takes the following form

$$A(T) = \frac{\langle T_{ocean} - T_{air} \rangle}{T_{ref}}. \tag{9}$$

The constant T_{ref} and the exponent m set the time scale over which $\hat{\tau}_{\mathrm{d}}$ returns to the value unity.

Figure 3 displays the evolution of the strength function for an exponent $m = 5$ and for three constant values of $A(T)$. The values of $A(T)$ used in this figure could correspond to a reference temperature $T_{ref} = 20°C$ and temperature differences between the ocean and atmosphere of $20°C$, $40°C$, and $60°C$ respectively. For these parameters the ice regains its strength within 3 to 11 days. Changes in the reference temperature change the typical length of time needed for the ice to regain its strength, and thus the model can be adjusted to fit observations. A key point is that this evolution equation allows the temperature to vary in any manner. Additionally, a new lead can be formed at any time based on the current strength. If either a completely refrozen lead whose strength has completely recovered, or a partially refrozen lead whose strength is still lower than the original value, is subject to new winds or ocean currents that cause it to reopen, then the strength recovery is reset and the process described above is repeated. We expect that if a lead opens and

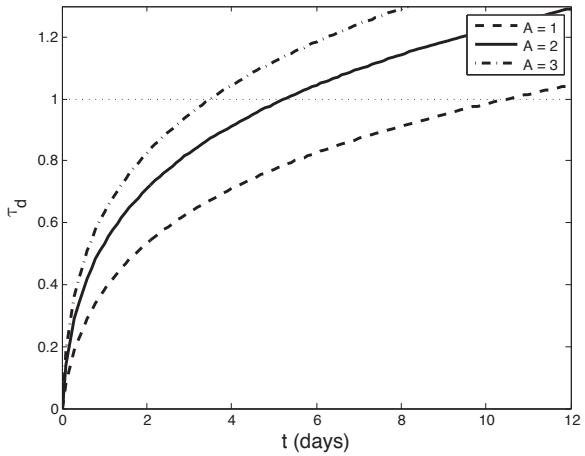

Figure 3: Time evolution of the strength parameter, $\tau_{\rm d}$, due to refreezing for constant ocean-air temperature differences. In practice, the parameter is not allowed to increase beyond unity.

closes repeatedly without refreezing then more ice is formed than if a lead opens and closes once with the ridged ice refreezing and regaining strength. These scenarios are explored through specific numeric examples in the next section.

4. Numeric Examples

In order to illustrate the behavior of the elastic-decohesive constitutive model with and without ice strengthening due to refreezing, we perform a simple calculation using the Material-Point Method (MPM). MPM is a numerical technique that combines Lagrangian particles with a background grid (Sulsky et al., 1994, 1995). A description of the application of MPM to sea ice is given in Sulsky et al. (2007) and Sulsky and Peterson (2011). The Lagrangian particles, or material points, carry mass, velocity, stress, ice thickness, and other material parameters and internal variables for the constitutive and thermodynamic models, as well as the thickness distribution. This allows for these quantities to be transported with the material motion in a natural manner. Material-point properties are mapped to the background grid for the solution of the momentum equation at each time step. The model used in this analysis combines the elastic-decohesive constitutive model used in the momentum equation for the ice dynamics, with an energy conserving thermodynamic implementation for ice growth and melt, and a five cateogry ice thickness distribution incorporating ridging. Governing equations for each of these components are found in Appendix A.

For the example calculation a block of ice 1050 km long and 600 km wide with an initial region of decohesion down the center, at $x = 0$ km, is forced by cyclic atmospheric winds. The computational domain is larger than the block of ice and is divided into a 1150 $\times$ 700 km background grid, which is composed of square cells of dimension 50 km. The ice region contained within the background grid is made up of material points. The region of initially weakened ice in a line through the center of the ice region is initialized by setting the normalized decohesion opening (u_n/u_0) equal to 0.8 and with the normal to the crack surface

set to the x-direction. Therefore, the initial strength function is $\hat{f}_n = 0.2$ along this line. An overview of the computational domain displaying initial values of the average ice thickness and normalized decohesion opening magnitude are shown in Figure 4. The initial average ice thickness is approximately 2.6 m for each material point and is calculated by summing over the five ice thickness categories at each material point. The parameters used in the decohesion algorithm are given in Table 1. We do not include a closing force in these simulations since ice does not grow sufficiently in open leads over five days to significantly impede motion.

The simulations are run for three months with a time step of 100 seconds. For the refreezing algorithm, the parameters chosen result in a strength evolution over time as shown in Figure 3 with $A = 2$. This value allows stationary ice to regain its strength in about five days. Note that the parameter A depends, in general, on the temperature difference between the ocean and the atmosphere and would therefore vary seasonally over a longer calculation. The atmospheric winds are set to pull then push the block of ice in the

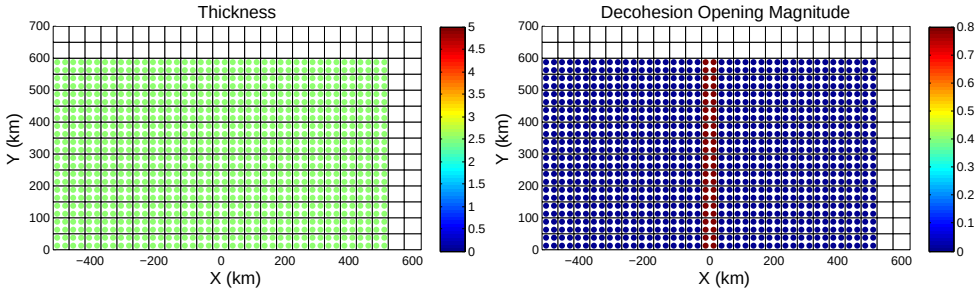

(a) (b)

Figure 4: Initial (a) ice thickness in meters and (b) normalized decohesion opening.

Table 1: Decohesion parameters used in the simulations.

Variable	Value	Description
τ_{nf}	2.5 KPa	tensile strength
τ_{sm}	6.0 KPa	shear strength
f_c'	12.5 KPa	compressive strength
u_0	4 km	minimum decohesion opening
σ_g	0	resultant stress component
m	5	exponent in strength factor

horizontal direction to open and close the crack down the center. This forcing is accomplished by setting the wind velocity to cycle, putting the ice in tension for a period of 5 days, compressing the ice for 10 days, and pausing for 10 day intervals of zero velocity between the active periods to allow for ice growth. A plot of the velocity cycle as a function of time for a point on the right side of the domain for the first set of simulations is shown in Figure 5a and a plot of the atmospheric wind velocity over the domain on day two is shown in Figure 5b. The ocean current is assumed to be zero, but an ocean drag depending on the ice velocity is still applied. The atmospheric and oceanic forcing has a magnitude consistent with typical forcing over winter months in the Arctic. The values for the oceanic and atmospheric forcing parameters are given in Table 2.

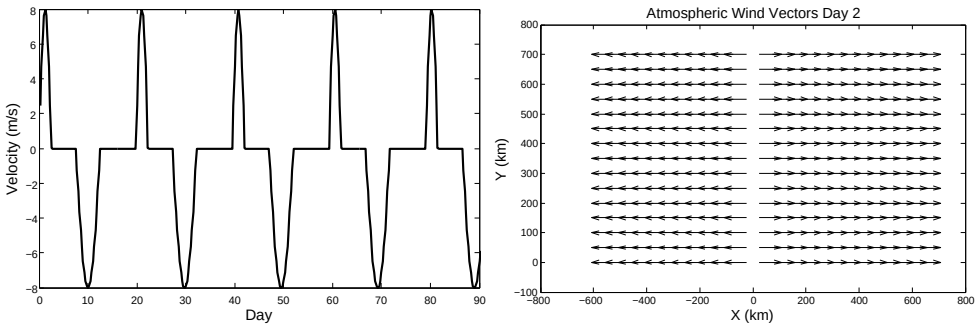

(a) (b)

Figure 5: (a) Atmospheric wind in the x direction as a function of time for a point to the right of the center of the block of ice. For points to the left of the center the wind velocity is equal and opposite. (b) Atmospheric wind vectors over the calculation domain on day 2 near the peak of the velocity cycle.

Table 2: Atmospheric and Oceanic Forcing.

Variable	Value	Description
F_{lw}	187.5 W/m^2	long wave flux
F_{sw}	0 W/m^2	short wave flux
T_{air}	-38 $^\circ C$	air temperature
Q	5 $\times 10^{-5}$	specific humidity
F_{snow}	6 $\times 10^{-6}$	snow flux (precipitation)
SST	-1.96 $^\circ C$	sea surface temperature
SSS	32 ppt	sea surface salinity

The different results produced in the simulations with and without a refreezing algorithm can be seen by plotting the normalized decohesion opening in the x direction for a point in the center of the ice domain as a function of time, as shown in Figure 6a. A material point is chosen in the initially weakened ice and its decohesion history is displayed in the figure. The point starts with a normalized decohesion opening equal to 0.8. Without refreezing, the ice can freely open and close and the decohesion opening cycles in response to the cyclic wind. The lead opens to a scaled value of 6 over the first 5 days, stays roughly constant over the next 5 days as the winds die down, and then closes within 5 days when the winds reverse. Since the ice is still fractured, when the wind changes, the lead can reopen and repeat the previous pattern. If refreezing is added, the first tension and compression cycle is identical. However, once the ice has compressed in the simulation with refreezing, the crack heals so that strength is regained over the ten days between the last compression portion of the cycle and the new tension portion of the cycle. Once this happens, the forcing in this simulation is never enough to reinitiate decohesion and the lead does not reopen. Therefore, on day 15 in Figure 6a the calculations begin to differ such that the ice with strength recovery is no longer able to pull apart under the given tension. The corresponding evolution of the strength factor is shown in Figure 6b. Without refreezing, the strength factor starts at 0.2 and then decreases to zero as the lead opens. The strength factor then remains at zero for the duration of the simulation. With refreezing, the strength factor recovers from zero back to one and the ice remains at full strength for the duration of the simulation. Note that the strength factor is only nonzero for points that have previously undergone decohesion and have

closed sufficiently to allow refreezing.

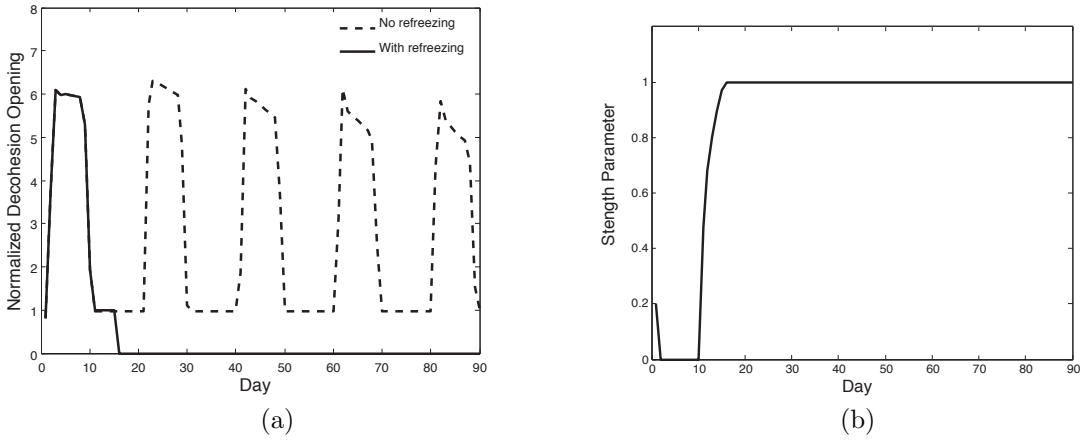

Figure 6: (a) Normalized decohesion opening as a function of time for a point in the center of the initial lead. The dashed line is for the case of no refreezing and the solid line allows refreezing and strength recovery. (b) Evolution of the strength factor as a function of time when refreezing is allowed, for the same point.

To examine how the refreezing algorithm effects ice production within a lead, we examine the average thickness for a point near the center of the ice domain and plot it as a function of time in Figure 7. The dashed line in the figure is the original model where the ice does not refreeze. The average thickness cycles with the applied atmospheric winds. When the winds pull the ice apart, open water is created, and the average thickness goes down. When the winds compress the ice, ridges form and the average thickness goes up. Over time, this cyclic motion increases the peak average thickness. However, ice growth is also affected by thermodynamics. Another simulation, labeled in Figure 7 as "No atmospheric wind" and plotted with a dotted line, is run to determine the ice growth in the case of zero velocity. In this simulation ice grows only due to thermodynamic processes since ridging due to ice deformation does not occur. The increase in peak thickness due to opening and closing of a lead and ridging ice, outpaces purely thermodynamic growth. Finally, in the case where refreezing is allowed, an initial ridge is formed during the first compressive cycle and then that ice increases slowly in thickness commensurate with thermodynamic freezing.

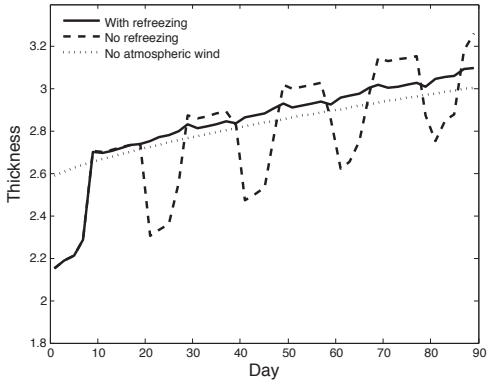

Figure 7: Thickness at a point near the center of the ice domain for three cases: with refreezing, no refreezing, and without atmospheric winds.

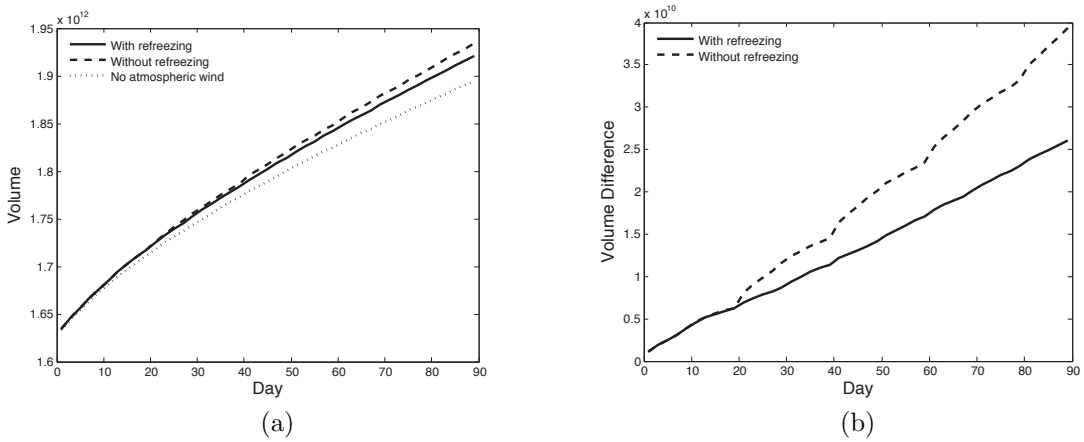

Figure 8: Ice volume versus time over the entire ice domain (a) for three cases: refreezing, original formulation, and no atmospheric winds and (b) for the refreezing and original formulation, with the thermodynamic thickness subtracted in each case.

The total volume of ice is also altered by the refreezing algorithm. The total ice volume is the area times the thickness, summed over the domain and is shown in Figure 8a as a function of time. The volume is increasing over time with and without refreezing, and without ice motion. To see the impact of refreezing a lead more clearly, the volume increase due to thermodynamic freezing is subtracted using the simulation with no atmospheric wind. Thus, Figure 8b measures the change in volume due only to ice dynamics. Clearly, the continued opening and closing of a lead causes an increase in ice volume as ice forms in the lead and is crushed into a ridge with each cycle. This increase in ice volume is larger by about 50% than the ice volume formed when the lead refreezes and does not reopen.

The thickness distributions at a point near the center of the domain for each of the cases previously considered are shown in Figure 9. Note that at the final time the thickness distribution without refreezing is shifted more towards thicker ice. This result is consistent with the average thickness over the domain being larger without refreezing. The thickness distribution when refreezing is allowed is more similar to the simulation that only produces ice through thermodynamics. Again, this picture is to be expected based on the calculations of ice thickness and volume changes.

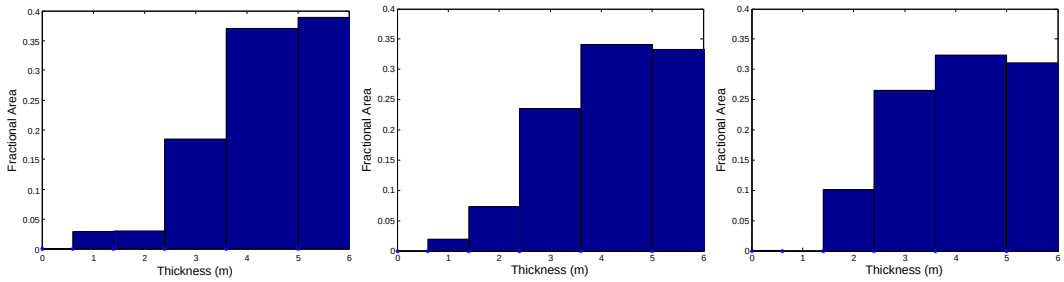

Figure 9: Ice thickness distribution at the final time for (a) with no refreezing, (b) with refreezing, and (c) with no atmospheric wind.

5. Summary

An elastic-decohesive model was developed to predict lead opening and the orientation of the lead in simulations of Arctic sea ice. In previous work, the model was shown to reproduce qualitative and statistical properties of lead formation in a regional study of the Beaufort Sea. This paper suggests modification to the model in order to add two important elements for predicting the closure of leads and the formation of fresh ice. First, the strength of fresh ice in compression has been added to account for the resistance of fresh ice when the gap making up the surfaces of the lead closes. Second, an evolution equation is provided to model the recovery of strength of a closed lead due to refreezing within ridged ice. With a reversal of wind a ridge with no strength will open and fresh ice will form in the lead. However, with a recovery of strength, the ridge may not open and, consequently, no new ice is formed. This second aspect is particularly important for an accurate prediction of the formation of fresh ice in leads, and ultimately for correctly predicting ice production in climate simulations.

Two simulations were performed, with and without strength recovery due to refreezing. The parameters were chosen to bracket two possible extremes and to illustrate the contribution of refreezing to the ice model. In the first simulation, the strength is not allowed to recover. The lead can open and close without resistance. Repeated, cyclic opening and closing of the lead produces more ice relative to the second simulation where the strength of the ice recovers when a ridge is formed. The impact of the modified model on global Arctic simulations remains to be seen, and is the subject of future work.

Appendix A. Equations of Motion

The mathematical model of sea ice is derived from considering the balance of linear momentum which is expressed by the following equation (Hibler, 1979)

$$m\frac{d\mathbf{v}}{dt} = \mathbf{F}^{\text{int}} + \mathbf{F}^{\text{ext}}. \tag{A.1}$$

In this equation, the time derivative is a material-time derivative, $d/dt = \partial/\partial t + \mathbf{v}\cdot\nabla$, where $\mathbf{v} = \mathbf{v}(\mathbf{x}, t)$ is the velocity field associated with the point $\mathbf{x}$ at time t. This equation is derived by assuming the ice properties are constant through the thickness. Integration through the thickness leaves a two-dimensional equation describing motion in the plane of the ice. The quantity m is the ice mass per unit area, and $\mathbf{F}^{\text{int}} = \nabla\cdot\bar{h}\boldsymbol{\sigma}$ is the force due to variation in internal ice stress, given by the divergence of the stress tensor, $\boldsymbol{\sigma}$, times the ice thickness, $\bar{h}$. External forces are described by the vector $\mathbf{F}^{\text{ext}}$ which include Coriolis forces, air stress and water stress, and effects of sea surface tilt. Ice thickness can change due to the thermodynamic processes of melting and freezing, or mechanical processes such as lead or ridge formation. Since numeric climate simulations still must use large computational elements, within each element there is a distribution of ice thickness. The quantity $\bar{h}$ is the average thickness. A subgridscale model for the distribution of ice thickness, $g(\mathbf{x}, h, t)$, keeps track of the evolution of ice thickness within an element (Thorndike et al., 1975)

according to the equation

$$\frac{dg}{dt} + (\nabla \cdot \mathbf{v})g + \frac{\partial(fg)}{\partial h} = \psi. \tag{A.2}$$

The first two terms in this equation describe horizontal transport and the changes in thickness at a point due to ice motion. The third term expresses transport in thickness space, with $f = dh/dt$ being the rate at which thickness h changes due to thermodynamic processes. Finally, ψ, describes mechanical redistribution of ice and accounts for ridge formation in converging flow or the creation of open water in diverging flow. The ridging redistribution function described in Lipscomb et al. (2007) is used in our simulations. The local average ice thickness can be computed from the distribution by integration in thickness space

$$\bar{h} = \int_0^\infty hg \; dh. \tag{A.3}$$

Freezing and melting on the top and bottom surfaces is determined by solving a one dimensional heat equation for the temperature through the thickness (Maykut and Untersteiner, 1971; Bitz and Lipscomb, 1999). The coordinate in the direction perpendicular to the plane of the ice is labeled as the z coordinate and the heat equation is

$$\rho c \frac{dT}{dt} = \frac{\partial}{\partial z}\left(k \frac{\partial T}{\partial z}\right) + \bar{\kappa} I_0 \mathrm{e}^{-\bar{\kappa} z}. \tag{A.4}$$

The heat capacity, c, and conductivity, k, are functions of temperature and salinity, where the salinity is given by a fixed profile depending on the vertical coordinate (Bitz and Lipscomb, 1999). The quantity $\bar{\kappa}$ is the extinction coefficient, and I_0 is the solar radiation that penetrates the upper surface. To obtain the change in thickness of the ice due to thermodynamic forcing the following balance of flux equations must be solved at the atmosphere and ocean interfaces

$$\begin{aligned} F_w - k\frac{\partial T}{\partial z} &= -q\frac{dh}{dt} \\ F_a + k\frac{\partial T}{\partial z} &= -q\frac{dh}{dt} \end{aligned} \tag{A.5}$$

where the enthalpy, q, is also dependent on the temperature and salinity. Note that dh/dt at each surface is summed to obtain the rate of change in thickness, f, in the ice thickness distribution equation, Equation A.2. The flux at the ocean interface, F_w, is simply the heat flux from the ocean to the ice. The net flux at the atmosphere interface, F_a, is a combination of flux terms as shown in Equation (A.6). It includes shortwave flux due to solar radiation, F_R, minus the fraction which is reflected based on the albedo of the surface, α, and the fraction that is transmitted through the ice, I_0. It additionally includes the downward longwave flux due to atmospheric heating, F_L, and the upward longwave flux from the ice surface, which is defined in terms of the surface temperature, T_0, the Stefan-Boltzmann constant, σ, and the longwave emissivity of the surface, ϵ_L,. The final terms in the balance are the flux of sensible heat, F_s, and the flux of latent heat, F_l

$$F_a = F_R(1-\alpha) - I_0 + F_L - \epsilon_L \sigma T_0^4 + F_s + F_l. \tag{A.6}$$

In order to complete the mathematical description, a constitutive model for the stress is required. This model is the topic of the main body of the paper.

Appendix B. Acknowledgements

The authors wish to acknowledge with fondness and appreciation that this work was initiated because of the persistence of Max D. Coon whose extensive knowledge of Arctic ice provided the insight on which many aspects of the models described in this paper are based. This work was partially supported by the National Science Foundation under grant ARC-1023667. Additional support for KP from the NNSA Climate Modeling and Carbon Measurement project and a Laboratory Directed Research and Development award are gratefully acknowledged.

References

Bitz, C. M., Lipscomb, W. H., 1999. An energy-conserving thermodynamic model of sea ice. Journal of Geophysical Research 104 (C7), 15669–15677.

Hibler, W. D., 1979. A dynamic thermodynamic sea ice model. Journal of Physical Oceanography 9, 815–845.

Lipscomb, W. H., Hunke, E. C., Maslowski, W., Jakacki, J., 2007. Ridging, strength, and stability in high-resolution sea ice models. Journal of Geophysical Research 112, C03S91.

Maykut, G. A., Untersteiner, N., 1971. Some results from a time-dependent thermodynamic model of sea ice. Journal of Geophysical Research 76 (6), 1550–1575.

Schreyer, H., Monday, L., Sulsky, D., Coon, M., Kwok, R., 2006. Elastic-decohesive constitutive model for sea ice. Journal of Geophysical Research 111, C11S26.

Schulson, E. M., 2004. Compressive shear faults within arctic sea ice: Fracture on scales large and small. Journal of Geophysical Research 109, C07016.

Sulsky, D., Chen, Z., Schreyer, H., 1994. A particle method for history-dependent materials. Computer Methods in Applied Mechanics and Engineering 118, 179–196.

Sulsky, D., Peterson, K., 2011. Towards a new model of Arctic sea ice. Physica D submitted.

Sulsky, D., Schreyer, H., Peterson, K., Coon, M., Kwok, R., 2007. Using the material-point method to model sea ice dynamics. Journal of Geophysical Research 112, C02S90.

Sulsky, D., Zhou, S., Schreyer, H., 1995. Application of a particle-in-cell method to solid mechanics. Computer Physics Communications 87, 236–252.

Thorndike, A., Rothrock, D., Maykut, G., Colony, R., November 1975. The thickness distribution of seaice. Journal of Geophysical Research 80 (33), 4501–4513.